Effect of the Temperature in Water Adsorption onto Sub-Bituminous Coal

Esteban A. Taborda[1], Camilo A. Franco Ariza[1], William A. Jurado[2], Nashaat N. Nassar[3] and Farid B. Cortés[1,*]

[1] Grupo de Investigación en Yacimientos de Hidrocarburos, Facultad de Minas, Universidad Nacional de Colombia Sede Medellín, Kra 80 No. 65-223, Medellín, Colombia. Email: fbcortes@unal.edu.co.

[2] Departamento de Optimización de Procesos, Grupo ARGOS S.A, Colombia.

[3] Department of Chemical and Petroleum Engineering, University of Calgary, 2500 University Drive NW, Calgary, Alberta, Canada. Email: nassar@ucalgary.ca, Fax: +14032103973, Phone: +14032109772

Abstract

The presence of water in coal presents a technological challenge for its industrial use in energetic processes. Therefore, this study aims to study the temperature effect on the water adsorption onto coals. A Colombian bituminous coal was used as sample. The coal was characterized by nitrogen adsorption at 77 K (S_{BET}), Scanning electron microscopy (SEM), Fourier transform infrared (FT-IR) spectroscopy, elemental analysis (C-H-N elemental). The results showed that the water uptake increased as the vapor pressure increased. The Talu and Meunier model [1] was used to fit the adsorption isotherms, and the mean square root error (MSRE%) was lower than 10%. Additionally, the Gibbs free energy was found to have negative values, which corroborates the spontaneous adsorption process.

KEYWORDS

Adsorption, Coal, Isotherm, Water Uptake

1. Introduction

Coal is the most abundant fossil fuel on earth and is one of the main energy resources [2]. Global coal production is expected to increase by 30% and reach a maximum between 2020 and 2050 [2, 3]. Colombia has been shown to have the largest coal reserves in South America and is ranked eleventh globally [2] [2-4]. Nearly 85% of global coal reserves correspond to sub-bituminous and brown coals [2, 3]. Both of these coal types have active sites resulting in high water content due to their high affinity for polar molecules [5, 6]. The presence of water in coals presents several challenges for its application, as follows: 1) The risk for spontaneous combustion increases due to the oxidation of carbonaceous material in the coal at room temperature. This occurs when the coal is exposed to air and undergoes exothermic chemisorption of oxygen. Large coal stockpiles, especially those stored for long periods, may develop hot spots because of self-heating [7-9] caused by the adsorption/desorption of water on coal [10]; 2) The industrial costs for coal transportation have increased; and 3) A high amount of energy is required for coal drying via the thermal processes. The amount of water present in the coal is obtained naturally and from the chemical conversion of hydrogen (in the fuel) to water, which reflects the net heating value (NHV) of the coal [11]. The goal of this study is evaluate the temperature effect on the adsorption of water onto Colombian sub-bituminous coal. Different water adsorption isotherms were obtained at 21°C, 40°C and 50°C. The isotherms were phenomenologically described by the Talu and Meunier model for understanding the behavior of auto-associative molecules like water on coal [1]. Coal sample considered in this study were characterized using FTIR analysis, elemental analysis (C-H-N), Brunauer–Emmett–Teller (BET) surface area analysis by nitrogen physisorption at 77 K and NHV. Additionally, the values of the thermodynamic properties of water adsorption on coal were calculated.

2. Experiments

2.1 Coal preparation

A coal sample was obtained from the Cordoba region in northwestern Colombia and was used in this study. The coal sample preparation was performed by separating and quartering the sample four times. The particle size was subsequently reduced to approximately 250 mm using a jaw crusher and a ball mill, according to ASTM D2013-01 method. The coal was then dried in air at 120°C for 12 h and was transferred on a dewatering system to reach room temperature.

2.2 Coal characterization

The coal samples were characterized before and after impregnation. Elemental analysis was performed using a 5000A TOC (CHN Shimadzu, Japan) for obtaining C-H-N elements; the oxygen element was obtained by difference. N2 physisorption at 77 K was performed using an ASAP 2010 (Micromeritics, USA). The surface area (SBET) was obtained after degassing the sample for approximately 12 h at 140°C under high vacuum (10-6 mbar). The SBET was estimated using the Brunauer, Emmett and Teller (BET) method [12-14]. The minimum limit for this instrument to reliably detect surface area is 1 m^2/g. To determine the functional groups present in the coal, each sample was characterized by infrared spectroscopy (IRAffinity-1S Shimadzu, Japan) [15-17]. Scanning electron microscope (JSM-5910JL, JEOL Japan) was used to obtain images of selected samples to confirm their non-porous structure.

2.3 Adsorption isotherms

The static thermogravimetric method was used for the construction of the adsorption isotherm at 21, 30, 40 and 50°C. This method involves determining the weight gain of the coal subjected to different water activities (Aw) at a defined temperature. Containers with eight supersaturated saline solutions that provided a range of water activity between 0.113 and 0.90 (Table 1) were placed in an oven at each temperature for 24 h. After saline solutions preparation, the activity was continuously measured until a constant value was reached. Then, 0.5 g sample of the coal was placed inside the eight containers until equilibrium is reached. The coal sample was weighed every 8 h with an analytical balance (OHAUS – accuracy of 0.0001

Table 1. Hygroscopic salt solutions to control water activity (Aw)

Salt	K_{ps} (g/100 ml H_2O)	Aw = P/P^{sat}
Lithium Chloride (LiCl)	83.2	0.113
Calcium Chloride ($CaCl_2$)	74.5	0.295
Magnesium Chloride ($MgCl_2$)	54.6	0.328
Potassium Carbonate (K_2CO_3)	112	0.432
Sodium Bromide (NaBr)	90.5	0.577
Sodium Nitrite ($NaNO_2$)	80.8	0.654
Sodium Chloride (NaCl)	39.8	0.753
Potassium Chloride (KCl)	34.2	0.843

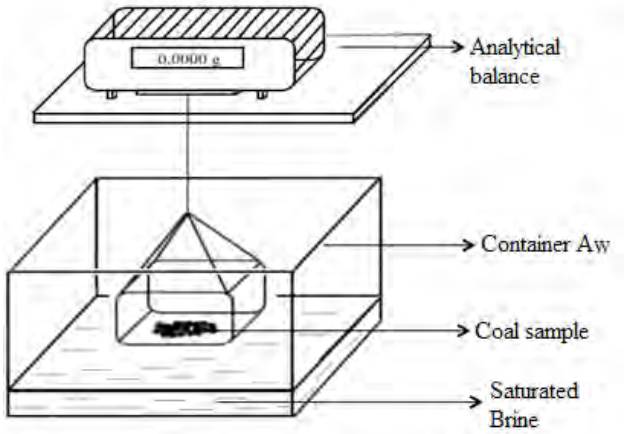

Figure 1. Schematic representation of the experimental set-up for adsorption isotherms construction.

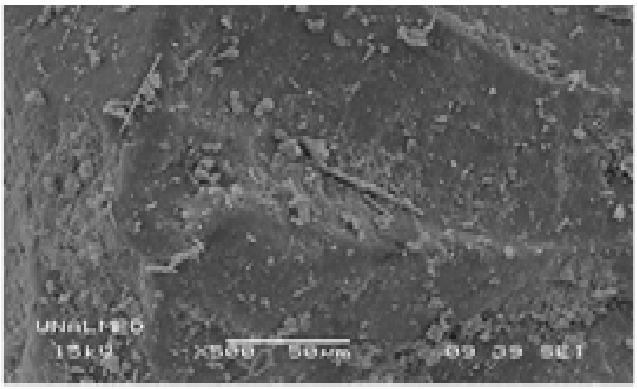

Figure 2. SEM images for selected coal sample.

Table 2. Elemental analysis (i.e., C-H-O-N) and estimated surface area.

Material	%Carbon (wt% C)	%Hydrogen (wt% H)	%Nitrogen (wt% N)	%Oxygen (wt% O)	O/C	H/C	S_{BET} (m^2/g)
Coal	64.79	5.15	1.96	28.11	0.43	0.079	4.94

g) until the sample weight did not vary by more than 1%. This procedure was performed by triplicated to confirm reproducibility, and standard deviations were calculated and presented as error bars on the isotherm figures. Finally, the amount of adsorbed water was estimated by calculating the difference between the initial and final sample weight. Water uptake (N_{ads}) was calculated as mg of water per g of dry coal [14, 18-25]. Figure 1 shows a schematic representation of the experimental setup. Table 1 shows the hygroscopic salts used to condition each system to the desired water activity.

3. Results and discussions

3.1 Samples characterization

Figure 2 shows scanning electron microscopy (SEM) images of coal. Accordingly, it seems that coal have a non-porous structure. Table 2 shows that the surface area (S_{BET}) of the coal. In addition, the low value of S_{BET} again supports that the materials are non-porous.

Table 2 also shows the elemental analysis of the coal samples.

3.2 Adsorption isotherms

Figure 3 shows the adsorption isotherm of water on coal at 21°C for a water activity between 0.10-0.90. The adsorption isotherms exhibited Type III behavior according to the IUPAC classification [1, 5]. The adsorption increased with increasing water activity. These findings are in good agreement with the available coal/water adsorption studies [23, 26-32]. The amount of water vapor in the sorption container increased due to increased vapor pressure (water activity). Collisions with the sample surface were highly favored, leading to a higher adsorbed amount. The resulting shape of the water sorption isotherm indicates a low affinity between the adsorbate and adsorbent, which mainly occurred at a low relative humidity (water activity). The behavior of the isotherm shows different interactions, including the water interaction with the active sites, along with multilayer adsorbed moisture on the surface of coal (Figure 3).

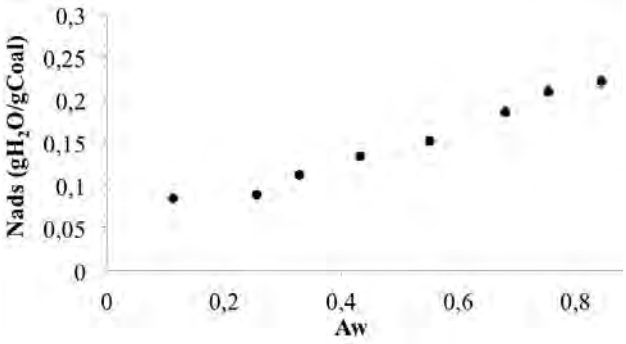

Figure 3. Water adsorption isotherm onto coal at 21°C.

The IR spectroscopy analysis shown in Figure 6 for sample after adsorption at Aw = 0.84. As seen, the signal near the 3300 cm^{-1} region indicates the presence of water [33]. It can be also seen that a signal intensity at approximately 3300 cm^{-1}. This is also representative of weather conditions in which water changes its intensity according to the sorption isotherm.

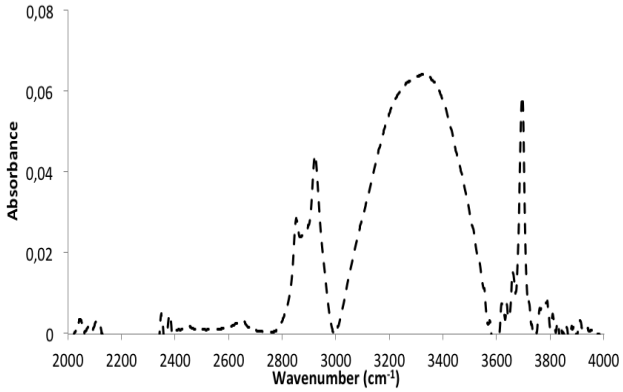

Figure 4. IR spectra for coal after adsorption at Aw = 0.84.

Adsorption isotherm were modeled using the Talu and Meunier model [1]. Talu and Meunier model [1] can be expressed as a general theory for the adsorption of self-associating molecules over solid structures. The approach is similar to the "*chemical*" interpretation of *non*-ideal vapor and liquid phases. The theory can explain the behavior of the Types I to V isotherms, including Type III isotherms characteristic of non-porous adsorbents, as it is the case of this work. Isothermal data are dependent on only three parameters: the inverse of Henry's law constant, the saturation capacity and the reaction constant for "cluster" [1]. The model is described as follows:

$$P = \frac{H\psi}{(1+K\psi)} Exp(\frac{\psi}{Nm}) \quad (1)$$

$$\psi = \frac{-1+\sqrt{(1+4K\varepsilon}}{2K} \quad (2)$$

$$\varepsilon = \frac{N_m N}{(N_m - \mathrm{N})} \quad (3)$$

where, *N (g/g)* is the adsorbed amount, N_m *(g/g)* is the saturation amount adsorbed by the monomer, *K (g/g)* is the reaction constant, *P (kPa)* is the equilibrium pressure, and *H (kPa)* is the Henry's law constant.

Figure 5 shows the comparison between experimental data and Talu and Meunier model fitting. Table 3 lists the values of the obtained parameters of the Talu and Meunier model. The parameter values are in agreement with the characteristics of the coals in which the *K* value is high. This indicates a rapid association of water molecules once the primary sites are occupied and is similar to the behavior described by the adsorption isotherms. On the other hand, the *H* values are also high (inverse of the common Henry's law constant), indicating that the steep rise in the water isotherm is delayed. Higher values of the *H* parameter indicate lower affinity of the water molecules for being in the adsorbed phase. The active sites are in locations that are not easily accessible to water. Low *K* values indicate that the primary sites are in widely varying space environments, resulting in a broadened step in the isotherm, which starts at lower pressures [1]. The differences between the N_m values for different coals simply correspond to the available adsorption space. This trend is also observed in the behavior of the isotherms (Figure 7).

3.2.1 Effect of the temperature

Figure 5 shows the amount adsorbed of water onto coal at 21, 30, 40 and 50°C for the sample together with the Talu and Meunier model fitting. Figure 8 shows that water adsorption is dependent on the system temperature. A Type III behavior according to the IUPAC classification [34] was exhibited, suggesting a multilayer adsorption for all evaluated temperatures. At a low water activity of less than 0.3, the behavior is described by the adsorption of water on the energy sites because of the preference and affinity of molecules for these sites [5, 6]. At high activity, the water molecules tend to form clusters around the high-energy sites via associations with hydrogen [1]. As expected, the equilibrium water content increased with increasing water activity. Furthermore, the amount of water adsorbed decreases with temperature because the higher energy weakens the interaction forces between the adsorbate and the adsorbent, thus facilitating water desorption [14]. With the data obtained through the sorption equilibrium tests at different temperatures, it is possible to calculate the thermodynamic properties of sorption.

The parameters for the Talu and Meunier model [1] at different temperatures for coal show a behavior of *H* that is only temperature dependent, as shown Table 3. Higher values suggest that there is a lower affinity between adsorbate and adsorbent at Henry's region [1]. When the temperature increases, the interactions between the coal and water are weakened, thus the interaction forces are reduced by the temperature. The parameter N_m is related to the maximum amount adsorbed, an increase in temperature favors the desorption, for this reason this parameter value decreases as the temperature increases. The *K* parameter is related to the degree of aggregation of water molecules on the surface of the adsorbent, hence the lower the amount adsorbed the less aggregation on the active sites, for that reason the parameter *K* decreases as the temperature increases.

3.3 Thermodynamic properties

To further understand the effect of temperature on adsorption, the thermodynamic properties of sorption were calculated. The isosteric heat of adsorption is the amount of energy dissipated during the adsorption process [6, 35]. It can also be defined as the amount of energy required for desorption. This can be calculated trough the commonly used Clausius-Clapeyron equation [18, 19, 21, 22, 35-37]. The isosteric heat (Q_{isos}) of adsorption in units of Cal/g can be estimated based on the established equilibrium between the condensed phase and gas phase [14]. This is shown in eq. 3:

$$Q_{isos} = \left(\frac{v_n}{v_g} - 1\right) RZ \left(\frac{\partial \ln P}{\partial\left(\frac{1}{T}\right)}\right)_{Nads} \quad (4)$$

where *P (kPa)* and *T (K)* are equilibrium pressure and temperature, respectively. *R* is the universal gas constant, *Z* is the compressibility factor V_n *(m³/g)* and V_g *(m³/g)* are the partial volume of the adsorbed species and of the gas phase respectively.

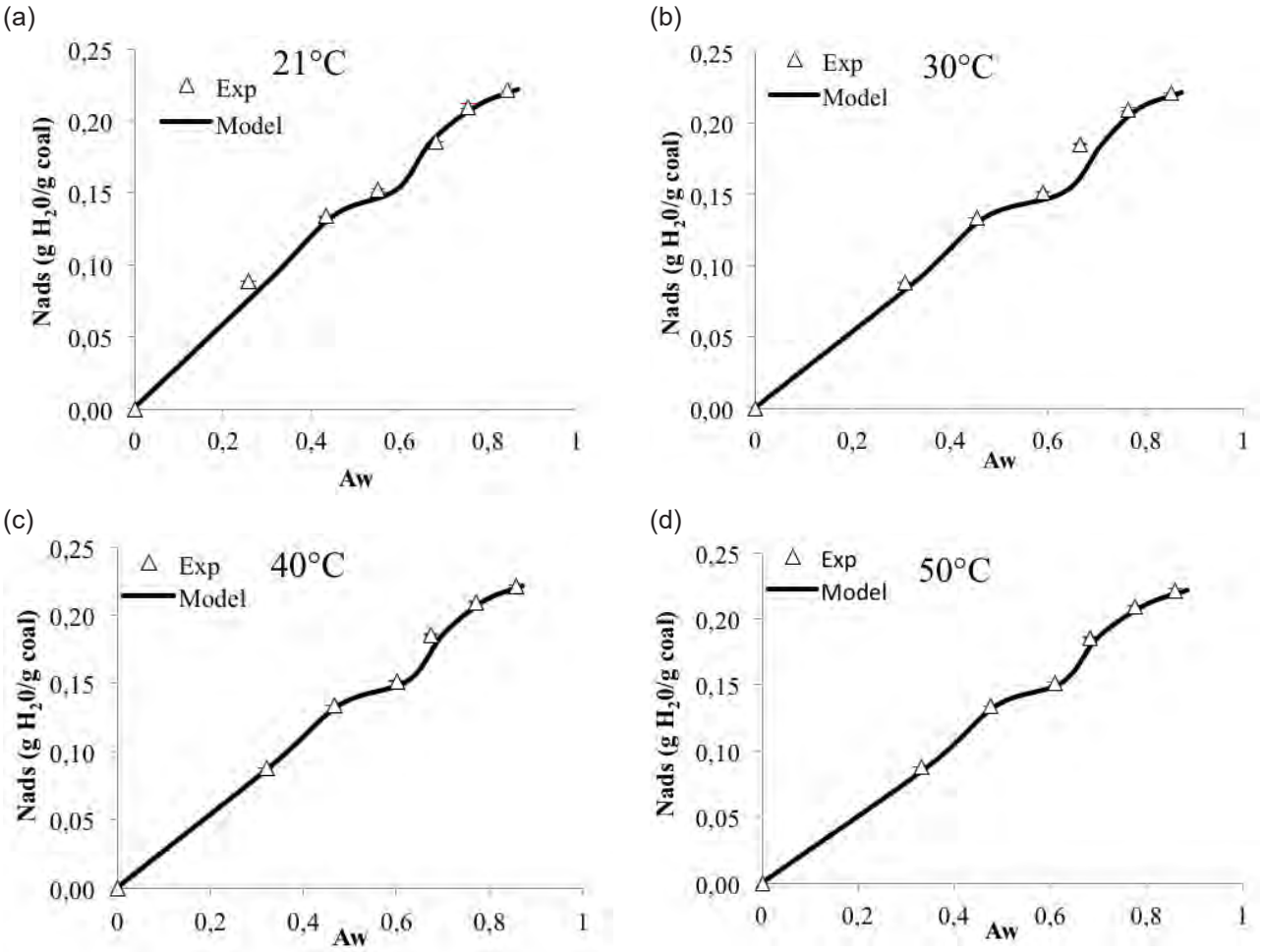

Figure 5. Water adsorption isotherms for coal at (a) 21°C, (b) 30°C, (c) 40°C and (d) 50°C

Table 3. Talu and Meunier model parameters for coal at all of the evaluated temperatures

Temperature	*H (kPa)*	*K (g/g)*	N_m *(g/g)*	MSRE (%)
21	18.5	16.9	0.18	7.45
30	82.5	14.9	0.16	8.12
40	140	14.4	0.15	7.15
50	215	13.5	0.14	4.25

Assuming an ideal gas case, for a constant value of N_{ads} eq. 4 can be simplified to eq. 5 [32]:

$$\left(\frac{\partial \ln P}{\partial\left(\frac{1}{T}\right)}\right)_{Nads} = -Q_{isos}/R \qquad (5)$$

From this equation, the isosteric heat can be calculated by determining the slope of the best fit line when ln(*P*) is plotted against *1/ T* [14, 18].

Figure 6 shows the isosteric heat of adsorption of water onto coal. *Qisos* decreases very slightly as function of *Nads* and remains nearly constant at approximately 600 Cal/g. This value is markedly lower than the isosteric heat for the virgin coal. It is suggested that the isosteric heat varies with water loadings to reveal lower heterogeneity energy of the adsorbent. This is because the high-energy points located on the coal surface reduce their energy intensity, then reducing their affinity to water.

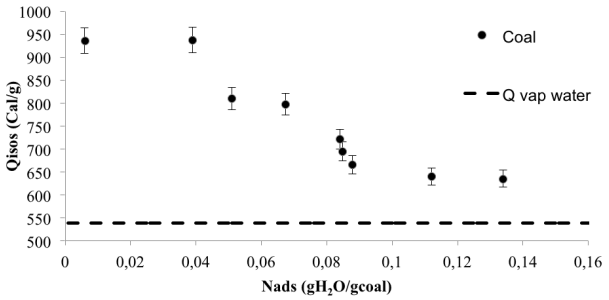

Figure 6. Isosteric heat of adsorption of water onto coal.

This result shows that the decrease very slightly in the energy heterogeneity of the adsorbent is because *Qisos* decreases as the amount of water adsorbed increases. This indicates that the coal surface presents highly energetic and closely related sites for polar compounds, such as water. This information is in agreement with the adsorption equilibrium in which a smaller amount is adsorbed onto the coal sample; therefore, a lower amount of energy is required to desorb the moisture. Figure 6 shows that the amount of energy required for the sample to dry to the desired

Table 4. Net heating value of coal impregnated with different concentrations of glycerol.

MATERIAL	HHV (Cal/g)	NHV (Cal/g)	NHV without the effect of glycerol (Cal/g)
Coal	5194 ± 77.91	4504 ± 67.56	4505 ± 67.56

moisture content is known. These data are important for the design of industrial scale dryers.

The Gibbs free energy of adsorption is a criterion that defines the feasibility and spontaneity of adsorption [13, 35]. The behavior, described by the adsorbed phase, is the same as the condensed phase. This is also known as the condensation approach and can be calculated using eq. 6 [13, 35].

$$\Delta G_0 = A = RTLn\left(\frac{P^0}{P}\right) \quad (6)$$

where, *A(Cal/g)* is the potential for molar adsorption, and *T(K)* and *P(KPa)* are the equilibrium temperature and pressure, respectively. The Gibbs free energy is calculated at a standard pressure "P^o".

Figure 7 shows the change in Gibbs free energy is a function of the adsorbed amount of water on selected samples. For all systems, the Gibbs free energy increases from a negative value to zero. This result demonstrates the thermodynamic consistency of the experimental data and confirms that the reaction is energetically spontaneous and heterogeneous. The data also show that the system is in agreement with the trends of isosteric heat, as reported in Figure 6.

More negative values of Gibbs free energy indicate an exothermic adsorption process; thus, the water molecules are stronger confined to the coal surface. The Gibbs free energy tends toward zero at adsorbed amounts greater than 0.04 g H_2O/g coal (percentages close to 4% moisture). This means that the process is less exothermic and that the strongly adsorbed water molecules are weakly bound to the surface of coal. This is because of the interaction of ambient water molecules with the water molecules already on the coal surface. Therefore, to reduce the moisture content of the treated sample from 10% to 4%, a small amount of energy is required to vaporize the water.

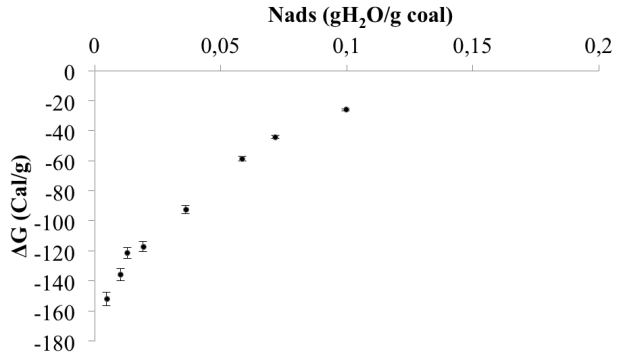

Figure 7. Relationship of Gibbs free energy and the adsorbed amount of water for coal.

3.4 Quality of coal

The heat of combustion of a fuel is commonly referred to as the higher heating value (HHV) or the caloric value. It is defined as the amount of heat released when a unit amount of the fuel is completely combusted. The heating value is a unique characteristic of each type of fuel. The lower heating value (LHV) is similarly defined, except that any water from combustion products is not condensed and remains as vapor. Thus, the LHV does not include the heat of vaporization of the produced water [31]. The relationship between the HHV and the LHV can be expressed as follows [11]:

$$NHV = HHV - Hv \quad (7)$$

For solid fuels (i.e., coal), it is typically expressed as follows [11]:

$$NHV = HHV - 10.55(W + 9Hg) \quad (8)$$

where:

H_v (Cal/g) is the vaporization heat, *NHV* (Cal/g) is the net heating value of coal, *HHV* (Cal/g) is the high heating value of coal in Cal/g, *W* (wt%) is the water amount in coal and *Hg* (wt%) hydrogen in coal.

Table 4 lists the estimated NHV of coal

4. CONCLUSIONS

The sorption equilibrium of water on a sample of sub-bituminous Colombian coal was obtained at 21, 30, 40 and 50°C through the static adsorption method. The results showed that the water uptake increased as the vapor pressure increased and decreases as temperature increases, with maximum water adsorbed was found at 21°C. The Talu and Meunier model was used to fit the adsorption isotherms, and the mean square root error (MSRE%) was lower than 10%. Additionally, the Gibbs free energy was found to have negative values, which corroborates the spontaneous adsorption process.

The thermodynamic properties in caloric value indicate lower costs per unit of energy and decreased transport costs compared with untreated coal.

5. ACKNOWLEDGMENTS

The authors acknowledge The Universidad Nacional de Colombia for logistical and financial support and ARGOS S.A.

REFERENCES

[1] Talu, O. and F. Meunier, Adsorption of associating molecules in micropores and application to water on carbon. AIChE journal, 1996. **42**(3): p. 809-819.

[2] Rempel, H., S. Schmidt, and U. Schwarz-Schampera, Reserves, resources and availability of energy resources. Hannover, Bundesanstalt für Geowissenschaften und Rohstoffe (BGR): www. bgr. bund. de, 2009.

[3] Rutledge, D., Hubbert's peak, the coal question, and climate change. Excel Workbook (permission is given to copy this work provided that attribution is given and the following web link is included). Website: http://rutledge. caltech. edu, 2007.

[4] Castro, J., Perspectivas de la demanda energética global.

Petrotecnia, 2011(1): p. 54-70.

[5] Dubinin, M., Inhomogeneous microporous structures of carbonaceous adsorbents. Carbon, 1981. **19**(4): p. 321-324.

[6] Dubinin, M. and V. Serpinsky, Isotherm equation for water vapor adsorption by microporous carbonaceous adsorbents. Carbon, 1981. **19**(5): p. 402-403.

[7] Bowes, P., Self-heating: evaluating and controlling the hazards. 1984: Department of the Environment, Building Research Establishment.

[8] Carras, J.N. and B.C. Young, Self-heating of coal and related materials: models, application and test methods. Progress in Energy and Combustion Science, 1994. **20**(1): p. 1-15.

[9] Nalbandian, H., Propensity of coal to self-heat. 2010: IEA Clean Coal Centre London.

[10] Kaymakci, E. and V. Didari, Relations between coal properties and spontaneous combustion parameters. Turkish Journal of Engineering and Environmental Sciences, 2002. **26**(1): p. 59-64.

[11] Gossman, D., Net Heating Values versus High Heating Values. GCI tech notes, 2011. **16**(1): p. 1.

[12] Brunauer, S., P.H. Emmett, and E. Teller, Adsorption of gases in multimolecular layers. Journal of the American chemical society, 1938. **60**(2): p. 309-319.

[13] Cortés, F., et al., Water adsorption on zeolite 13X: comparison of the two methods based on mass spectrometry and thermogravimetry. Adsorption, 2010. **16**(3): p. 141-146.

[14] Rouguerol, F., J. Rouguerol, and K. Sing, Adsorption by Powders and Porous Solid; Principles, Methodology and Applications. 1999, Academic Press, San Diego.

[15] Franco, C., et al., Water Remediation Based on Oil Adsorption Using Nanosilicates Functionalized with a Petroleum Vacuum Residue. Adsorption Science & Technology, 2014. **32**(2-3): p. 197-208.

[16] Franco, C.A., et al., Adsorption and Subsequent Oxidation of Colombian Asphaltenes onto Nickel and/or Palladium Oxide Supported on Fumed Silica Nanoparticles. Energy & Fuels, 2013. **27**(12): p. 7336-7347.

[17] Franco, C.A., N.N. Nassar, and F.B. Cortés, Removal of oil from oil-in-saltwater emulsions by adsorption onto nano-alumina functionalized with petroleum vacuum residue. Journal of colloid and interface science, 2014. **433**: p. 58-67.

[18] Comaposada, J., P. Gou, and J. Arnau, The effect of sodium chloride content and temperature on pork meat isotherms. Meat Science, 2000. **55**(3): p. 291-295.

[19] Vos, P.T. and T.P. Labuza, Technique for measurement of water activity in the high aw range. Journal of agricultural and food chemistry, 1974. **22**(2): p. 326-327.

[20] Coleman, R. Irreversible drying of carbonaceous fuels such as low-rank coals. in Fuel and Energy Abstracts. 1996. Elsevier.

[21] Cortés, F.B., V. López, and B.A. Rojano, Sorption properties of Cape gooseberry (Physalis peruviana L.). International Journal of Food Engineering, 2012. **8**(1).

[22] Davy, R., et al., Residual moisture reduction of coarse coal using air purging. 2. Pilot scale studies. Minerals engineering, 2001. **14**(6): p. 671-680.

[23] Nishino, J., Adsorption of water vapor and carbon dioxide at carboxylic functional groups on the surface of coal. Fuel, 2001. **80**(5): p. 757-764.

[24] OMAÑA, M., et al., Isotermas de sorción de agua en residuos de extracción de jugo de naranja. Biotecnología en el Sector Agropecuario y Agroindustrial, 2010. **8**(1): p. 61-67.

[25] Zapata, K., B.A. Rojano, and F.B. Cortés, Effect of Relative Humidity on the Antioxidant Activity of Spray-Dried Banana Passion Fruit (Passiflora Mollisima Baley)-Coated Pulp: Measurement of the Thermodynamic Properties of Sorption. Chemical Engineering Communications, 2015. **202**(3): p. 269-278.

[26] Allardice, D., et al., The characterisation of different forms of water in low rank coals and some hydrothermally dried products. Fuel, 2003. **82**(6): p. 661-667.

[27] Charrière, D. and P. Behra, Water sorption on coals. Journal of colloid and interface science, 2010. **344**(2): p. 460-467.

[28] Chen, X.D., A new water sorption equilibrium isotherm model. Food research international, 1997. **30**(10): p. 755-759.

[29] Karthikeyan, M., et al., Factors affecting quality of dried low-rank coals. Drying Technology, 2007. **25**(10): p. 1601-1611.

[30] Marchessault, R., Application of infra-red spectroscopy to cellulose and wood polysaccharides. Pure and Applied Chemistry, 1962. **5**(1-2): p. 107-130.

[31] McCain, W.D., The properties of petroleum fluids. 1990: PennWell Books.

[32] Shigehisa, T., T. Inoue, and H. Kumagai, Mathematical model of water sorption isotherms of UBC. Fuel Processing Technology, 2015. **131**: p. 133-141.

[33] Sing, K.S., Reporting physisorption data for gas/solid systems with special reference to the determination of surface area and porosity (Recommendations 1984). Pure and applied chemistry, 1985. **57**(4): p. 603-619.

[34] Peinter, P., M. Starsinic, and M. Coleman, Determination of functional groups in coal by fourier transform interferometry, fourier transform infrared spectroscopy. Academic Press, New York, 1985. **4**: p. 169.

[35] Soares, J.L., Desenvolvimento de novos adsorventes e processos híbridos em reforma catalítica por vapor de água. 2003.

[36] Cortes, F.B., B. Rojano, and F. Chejne Janna, Advantages and thermodynamic limitations of the experimental sorption isosteric method. Dyna, 2013. **80**(182): p. 155-162.

[37] Seifert, J. and G. Emig, Mikrostrukturuntersuchungen an porösen Feststoffen durch Physisorptionsmessungen. Chemie Ingenieur Technik, 1987. **59**(6): p. 475-484.